Plasma Density Profiling from Laser Diagnostics in FLASHForward

Lewis Dickson, University of Glasgow, Scotland

September 5, 2018

Abstract

The aim of the project was to produce a MATLAB script for calculating the plasma density distribution and investigating the laser characteristics in the FLASHForward Plasma Wakefield Accelerator at DESY. The project used the longitudinal laser diagnostic in the experiment to scan over the laser propagation path and produce intensity profile data of the beam at user defined locations within the scanning range. The project was successfully completed with the data analysis including the production of a laser intensity profile at each scanned position, the X and Y axis projections of these intensity profiles along with their corresponding σ_x and σ_y values, the calculation the M^2 value of the laser, and finally the calculation of the plasma density profile produced by the laser over the length of the plasma capillary within the experiment. All data taking and analysis is performed automatically with user input only required to select where the data is taken and how it is processed. All analysis was performed for the current argon gas set up. Code produced during the project and useful files such as background scans can be found at `https://github.com/wisky02/DESY`.

Contents

1 Introduction

Linear accelerators are necessary for high energy electron sources due to the issues with large synchrotron radiation produced in circular accelerators with light particles. However, due to the single pass of an accelerating gradient experienced by electron bunches in linear accelerators, these devices are limited in to energies that be achieved with conventional Radio-Frequency(RF) cavities. One method of combat this is to implement larger accelerating gradients. Plasma Wakefield Accelerators (PWFA) are a promising solution to this issue due to having accelerating gradients up to three orders of magnitude larger than conventional RF accelerating cavities[1]. For the acceptance of PWFA as a valid acceleration method it must produce beams of comparable quality to current technologies. PWFA is, however, in it infancy and so there are still several unsolved issues. This project aims to provide a means to analyse the plasma which plays a large role in the accelerating parameters. High-energy lasers are used for the ionising the argon gas into a plasma. Therefore, using the same diagnostics to used to collect the data to calculate the plasma density profile the laser characteristics can also be investigated. My project was coding based with time spent improving the script and measuring real data in the FLASHForward control room. I also became familiar with the JDDD interface used at DESY for controlling everything from cameras to motors.

2 Motivation and Aims of Summer Project

One of the major issues stopping PWFAs becoming a commonly used accelerating technique is their large emittance - the spread of electron trajectories on exiting the accelerator - of the accelerated beam. Reducing the emittance of the electron beam in PWFA experiments is a key hurdle to producing a high quality accelerated beam for use in free electron lasers (FEL) and, with even more stringent requirements, linear colliders. A suggested method to reduce this emittance is tailoring the plasma density distribution at the boundary between the plasma cell and the beam path vacuum. If a tailored plasma density profile is to be created, either separately or with the ionisation laser, an understanding of how the laser effects the plasma density is crucial. This project will thus focus on exploring how the measured ionising laser intensity profile in FLASHForward affects the plasma density within the plasma chamber. Further, for creating tailored plasma densities an understanding of the laser characteristics is required. In addition, it was shown at FACET that ultra-relativistic electron beams can be driven by neutral plasma columns[2]. Therefore, understanding the shape of the plasma distribution in relation to the electron beam location will be of interest in PWFA accelerators to account for these driving effects.

This project will explore relatively simple aspects of the laser such as the M^2 value of the beam. This investigation will be completed by a MATLAB script to take the data over the beam path using the longitudinal laser diagnostics at FLASHForward and analyse this data with minimal user input. The desired analysis for the laser are XY projections of intensity, σ_x and σ_y values, the M^2 value and for the plasma: the 3D plasma density

distribution.

3 Background

Here we will cover the basic concepts of a PWFA experiment and laser diagnostics as used within FLASHForward, the use of high-energy lasers for ionisation and how these are modelled through the ADK rate.

3.1 FLASHFoward

The FLASHForward facility is DESY's contribution to the understudied field of plasma wakefield accelerators. Using the 1.25 GeV FLASH electron beam as the drive beam for the PWFA experiment in the FLASH2 beam hall, FLASHForward aims to probe the issues stopping PWFA becoming a realistic method used in future particle accelerators. It also aims to demonstrate the feasibility of using beams accelerated through the plasma as a source for a free electron laser (FEL) which requires good beam quality from the accelerating cavity[3]. Whilst the setup of FLASHForward is complex the areas of interest in this project were the longitudinal beam diagnostics and how the measurements of the beam allowed the plasma density within the plasma cell to be modelled.

3.2 Longitudinal Laser Diagnostic

The properties of the laser have to be measured externally to the plasma cavity due to the hostile environment present. In FLASHForward the ionising laser is split with one half being directed to the plasma chamber for ionisation, whilst the other is propagated into the longitudinal laser diagnostic section of the experiment. The diagnostic beam is propagated the same distance as the ionising beam so that the beam measured in the diagnostic stage should be the same as if you were to measure directly in the plasma chamber. The use of a delay stage attached to an OWIS motor in the longitudinal beam diagnostic allows the path of the diagnostic laser to be lengthened or contracted. This allows effective scanning over the intensity profile of the ionising beam which is measured by a camera in the diagnostic stage. Being able to scan over the beam allows a three dimensional image of the laser intensities within the plasma cell to then be built. This data is then used to characterise the beam and calculate the plasma density profile.

4 Theory

4.1 Plasma Wakefield Acceleration

Whilst there are two main methods of producing the wakes within plasma only particle-driven Plasma Wakefield acceleration (PWFA) will be discussed. Laser driven wakefield acceleration (LWFA) is also investigated at DESY however I had no involvement in this. It should be noted that the laser used in FLASHForward is used for preionisation

purposes and not for producing the wakes required for acceleration as in LWFA experiments. Plasma Wakefield Acceleration is the utilisation of large longitudinal electric fields created within plasmas to accelerate particles. The two beams of interest in a PWFA experiment are the "drive" and "witness" beams. The wakefields within the plasma that provide the electric field are induced with the drive beam. Whilst FLASH-Forward utilises the electron beam from FLASH the method of exciting the plasma wake can also be achieved with proton beams as recently demonstrated in CERN's AWAKE experiment[4]. The simple requirement is that the particle drive beam be charged so that its electric field interacts with the plasma. In the case of FLASHForward the electric field of the electron drive beam repulses the electrons in the plasma. As these are approximately 2000 times lighter than the ions the latter do not move appreciably. This movement of the electrons leaves the ions unshielded and so the electrons are pulled back towards them by the electrostatic restoring force. This resulting periodic electron density perturbation causes the large longitudinal electric fields responsible for PWFAs high accelerating gradient. If no electrons are purposefully injected into the plasma wake, electrons within the plasma with the correct phase will experience an accelerating force and gain significant energies. Future techniques for injecting the electrons at the correct phase such as Trojan horse and plasma torch injection will require a combination of a low ionisation threshold (LIT) and high ionisation threshold (HIT) gases. The proposed mixture at FLASHForward is a hydrogen/helium mix respectively for LIT and HIT. Currently the FLASHForward set-up uses arcing to produce the plasma from argon gas. Because of this, argon gas variables are used throughout the simulations but it is noted in section 4.2.2 that this is easily changed.

4.2 Plasma Production by Laser Pulse

For the creation of the wakefields the particle beam must pass through a plasma so that the electrons are free to move and produce the wakes. Whilst the plasma is currently created in FLASHForward through the arcing of the argon neutral gas, future plans include the use of the high-energy laser for this purpose. Thus, the ionisation effects of the argon gas must be modelled by using the electromagnetic fields of the laser. In this project single ionisation was calculated for argon with ξ_i defined as the energy of the electron without the applied electric field from the laser normalised to the atomic energy scale.

Argon	Ionisation Number	ξ_i
	1	0.5794

4.2.1 Tunnelling Ionisation

At the electric field values produced by the ionisation laser at FLASHForward the relevant tunnelling mechanism is tunnelling ionisation. This is appropriate for as long as the electric field is below he critical electric field defined as: $E_{crit} = (\sqrt{2} - 1)|\xi_i^{\frac{3}{2}}|$. The bound electron's of an atom exist within the atomic electric potential produced from the

charged nuclei. The electric field of the laser pulse reduces the electric field experienced by the electron. The decrease in this potential increases the probability of the electron tunnelling from the atom thus producing an ion. The production of these electron-ion pairs (in the case of singular ionisation) is what forms the plasma.

4.2.2 Ammosov–Delone–Krainov Model

The Ammosov–Delone–Krainov model (ADK) [5] models the tunnelling ionisation of atoms in electromagnetic fields. The ADK rate can be calculated for arbitrary atoms knowing only the energy of the electron to be tunnelled and the charge of the ion after ionisation. Results for this method have been shown to agree well with numerical simulations for the case of hydrogen gas[6]. This was later used in Particle-in-cell simulations[7] and the method in the cited paper was used during the plasma density calculations performed in this project. Whilst their paper did not examine the effects of tunnelling ionisation in argon samples comparisons of the results seem reasonable.

The simplified ADK rate equation used for the plasma density calculation (eqn 1)

$$W(s^{-1}) = 1.52 * 10^{15} \frac{4^{n^* \xi_i(eV)}}{n^* \Gamma(2n^*)} \left(20.5 \frac{\xi_i^{\frac{3}{2}}(eV)}{E[GV/m]} \right)^{2n^*-1} \times exp\left(-6.83 \frac{\xi_i^{\frac{3}{2}}(eV)}{E[GV/m]} \right) \quad (1)$$

where ξ_i is the energy of the electron being ionised before the external electric field is present normalised to the atomic energy scales ($\approx 27.2eV$), E is the external electric field, n^* is the effective principle quantum number equal to $n^* = \frac{Z}{(2\xi_i)^{\frac{1}{2}}}$ where Z is the charge number after ionisation, and Γ is the Gamma function. It should be noted that the electric field from the laser pulse is given in giggavolts per meter.

The ADK rate is defined as the probability that an electron will be tunnel from the atom per unit time. The laser pulse is modelled as having a Gaussian wave packet and so when calculating the absolute ionisation of the plasma, the product of the ADK rate and the Gaussian wave packet are integrated over $\pm 3\sigma$ of the pulse time. This gives the dimensionless value of the number of ionisations and therefore the plasma density. The Gaussian wave-packet was defined by:

$$f(t) = \exp\left(\frac{-t^2}{2\tau^2} \right) \quad (2)$$

Where t is the time variable and τ is the pulse length defined to $35 * 10^{-15}$s.

The ADK rate is valid only under the critical electric field (defined in section 4.2.1) value as it only models tunnelling ionisation. At higher electric fields strengths the barrier suppression ionisation becomes dominant[8]. This value was calculated and found to be greater than the electric field present due to the ionising laser. The model accounts for this critical electric field through tunnelling ionisation rate decreasing at higher electric fields which should not be confused with a lower total ionisation. The effect simply comes from different sources of ionisation such as barrier suppression ionisation where the atomic potential is reduce such that it no longer binds the electron.
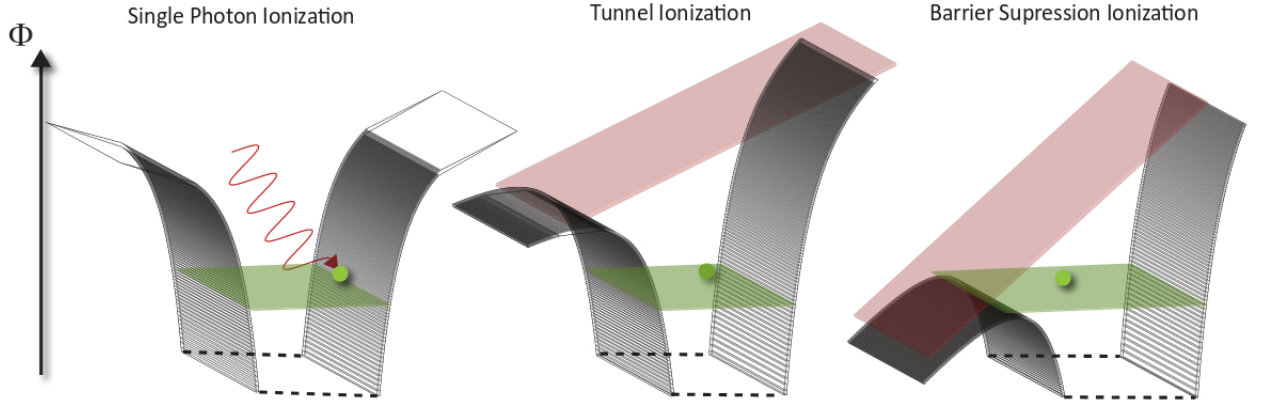
6

Figure 1: Figure extracted from [8]. The shaded black area indicates to atomic electrical potential. The green indicates the electron of interest's energy. Φ is the energy of the atomic potential. Tunnel Ionisation is the ionisation used in the calculation of the ADK rate (see section 4.2.2)

4.3 Beam Parameter Product and M^2 Beam Value

To measure the quality of the beam the method presented in [9] was followed. The initial step involved measuring the "second moment width" otherwise known as D4σ of the beam. The definition of this value is presented in equation 4 and is defined as four times the standard deviation of the beam. In the code this value was calculated in both the x and y direction so that the corresponding M^2 values in these directions could be calculated. This was necessary due to the asymmetry in the beam as can be seen in figure 5. The beam parameter product (BPP) is defined as "the product of beam radius (measured at the beam waist) and the beam divergence half-angle (measured in the far field)"[10]. The ratio of this value to that for a Gaussian beam of the same wavelength is defined as the M^2 value of the beam. This is a quantity used to characterise the quality of the laser beam. Here the value of the BPP is not calculated directly, as the data for the beam is fit to equation 3 to extract the quantities for the beam waist, beam waist position and M^2 value.

$$W^2(z) = W_0^2 + M^4 \left(\frac{\lambda}{\pi W_0} \right)^2 (z - z_0)^2 \tag{3}$$

Where

$$W^2(z) = \frac{(D4\sigma(z))^2}{2}$$

and W_0 is the beam waist, λ is the wavelength of the laser, z is the longitudinal position and z_0 is the longitudinal position of the beam waist. Further,

$$D4\sigma = 4\sigma = 4\sqrt{\frac{\int\limits_{-\infty}^{+\infty}\int\limits_{-\infty}^{+\infty} I(x,y)(x-\bar{x})^2\,dx\,dy}{\int\limits_{-\infty}^{+\infty}\int\limits_{-\infty}^{+\infty} I(x,y)\,dx\,dy}} \tag{4}$$

where,

$$\bar{x} = \frac{\int\limits_{-\infty}^{+\infty}\int\limits_{-\infty}^{+\infty} I(x,y)x\,dx\,dy}{\int\limits_{-\infty}^{+\infty}\int\limits_{-\infty}^{+\infty} I(x,y)\,dx\,dy}$$

Here "I" is the position dependent intensity. This same calculation was completed using "y" instead to calculate D4σ in the y direction.

4.4 JDDD

The use of the "Java DOOCS data Display" (JDDD) software at DESY allows the user to create control panels to easily interact with the experiments. The predefined commands for reading and writing information to the motors and sensors allowed the project to be completed within the allotted time frame. For that I am extremely grateful to those that worked to make JDDD and the FLASHForward panels so user-friendly. Using the self-explanatory "doocsread" and "doocswrite" commands allowed the taking of the data and the setting of the motor position to be controlled with single lines of code. Each camera is designated its own data readout data location where data is extracted using the "doocsread". This produces a struct of the image data where the pixel values were then extracted and used for the data analysis.

5 Code

The full MATLAB script created in this project can be found at the `https://github.com/wisky02/DESY`. The code had three main modes of function. The initial setting creates an example Gaussian distribution of the laser beam with intensities in the order of magnitude of the real data. The second setting allows the user to run the full script as intended by the project. This involves full data taking and control over the motor functions. Finally, a setting was scripted to allow the used to load in previously taken data for analysis in the many functions included. An overview of the code structure is presented in figure 2.

5.1 Control of Motor Stages

JDDD commands mentioned in section 4.4 allowed the user to quickly select which motor to be controlled and the desired movement to be initiated.
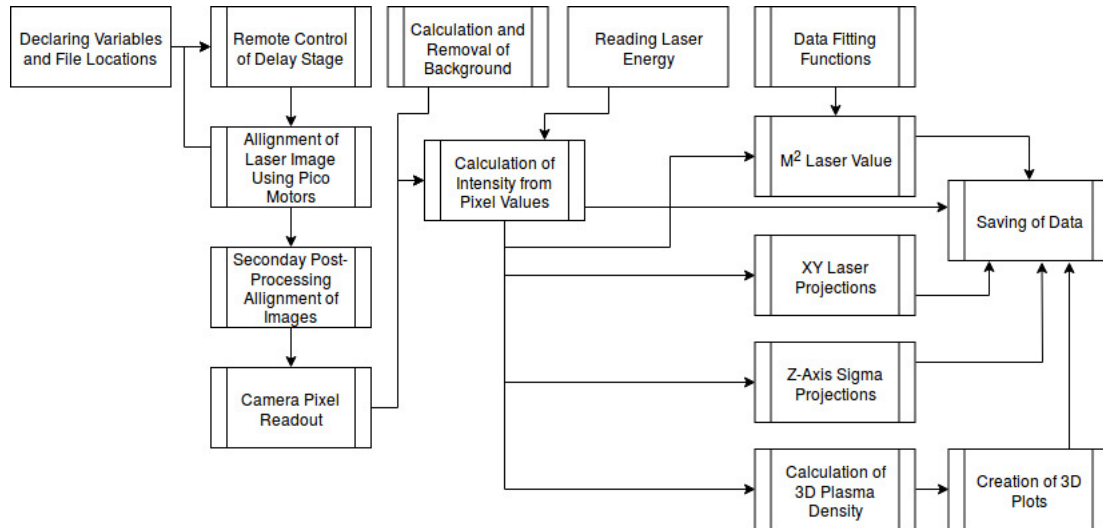
Figure 2: The figure displays the Gaussian intensity profile used for the example process in the code.

The OWIS motor on the delay stage was used to control the scanning of the Z-axis position of the beam. This allowed micrometer steps sizes through the beam. The OWIS motor has 3810000 steps with a step size of 1.05 μm as measured by Dr Knetsch. An important distinction between the control of the OWIS motors and that of the PICO motors is that the OWIS motor has an absolute zero position whilst the PICO motors zero will reset every time it is powered on. This means that the commands to the OWIS are always in absolute position whilst the movement of the PICO motors are given as relative movements. The control of the OWIS motor is initiated with the user input of a minimum and maximum scanning location along with the number of scans to be completed within this range.

The PICO motor stages provided the realignment of the focusing mirror after the delay stage was moved. This was necessary as the movement of the delay stage would drive the beam. To correct for this misalignment which would otherwise provide erroneous laser intensity data a single PICO motor was controlled in both the X and Y directions independently to refocus the beam to the centre of the camera. The PICO motor control revolves around the independent minimisation of the X and Y positions of the centroid of the intensity profile from the centre pixels of the image. This minimisation is given a tolerance difference for sake of speed which is what necessitates the used of a post processing image alignment function which is discussed in section 5.2. During testing it was noted that on some alignment loops this function would take up to a couple of minutes to optimise the location of the intensity profile. Whilst the step size of the motor was already proportional to the centroid's distance from the centre, the PICO motor was instructed to reduce the step size further after a given number of steps.

5.2 Post Processing Image Alignment

The post-processing image alignment function worked in a similar way to the PICO motor alignment function. However, as the image has absolute coordinates to work with the alignment could be centred in one step. The centroid of the image was again calculated and the difference between the centre of this image and the centroid used to move the image. The blank pixels at the edges of the intensity image were then filled with the average pixel background of the camera when no laser light is incident.

5.3 XY Laser Intensity Projections

Summing the measured intensities of the laser beam profile in the X and Y directions was useful to see the focus of the beam. It is noticeable from the results that in the Y axis the beam has an approximate Gaussian distribution whilst it is more heavily smeared in the X axis. This simple calculation was then plotted along side the laser intensity profile and used for the later calculations of the sigma value of the laser beam(see section 5.4). The green and red lines in figure 6 are simply for a visual representation of the beam and have been scaled to do this. Therefore only the projection plots above the image should be used for reference to absolute laser projection.

5.4 σ_x and σ_y Laser Calculation

The standard deviation of the laser pulse in the x and y direction were calculated from the axis projections of the laser beam intensity. These were then plotted along the spacial Z axis locations as measured through the movement of the OWIS motor. These values were then divided by the value of the images that they were extracted from to provide the coefficient of variation. This later technique was used in an attempt to find a possible beam waist which was sadly unsuccessful.

5.5 M^2 Laser Value Calculation

Diagnostic of the laser beam is necessary for understanding the characteristics and focus of the beam. These values were extracted through the fitting of the laser profile to the equation 3. The M^2 calculation was confirmed to be accurate in the case of the Gaussian used in the example returning values of M$_x^2$ = 1.232 M$_y^2$ = 1.232. The value is greater than that of a perfect Gaussian due to the example intensities being fit to the asymmetric grid which the real data was also plotted on.

5.6 Plasma Density Profile Calculation

The plasma density calculation was based of the time integrated ADK rate discussed in section 4.2.2. The laser wave packet was modelled as a Gaussian with a pulse length of 35 fs. The intensity image was multiplied by this wave packet and the result numerically integrated over ±3 sigma of the pulse length. Numerical integration was required due

to the lack of analytical solutions for the integration of the product of the ADK rate with the Gaussian wave-packet. The plasma density of each slice were then combined into a 3D model for the plasma density thus producing a plasma density profile over the scanned length of the laser.

Due to the flexibility of the ADK rate calculation (see section 4.2.2) should a different gas (or gas mixture) be used in the plasma cell only the charge after ionisation ,Z, and the normalised energy of the electron in the atom without the external field, ξ_i, need be altered. For gas mixtures, they would need to be calculated separately.

5.7 Saving of Data

Whilst being less exciting, the ordered saving and retrieval of data throughout the script, proved crucial in allowing the code to operate in the different settings. A short bash script was also created to create the directories necessary for saving the produced data and outputting these directories location so that the user can specify them in the code for saving purposes.

5.8 Gaussian Example Results

The Gaussian beam example is useful for evaluating the efficacy of the data analysis techniques and for troubleshooting plotting issues. A Gaussian beam intensity is defined for each scanning location. This simplified code places the same intensity distribution at all points so is far from realistic. Whilst the centre of the Gaussian was fixed at the centre of the image the sigma value for the beam was arbitrary and set to provide an intensity image which spanned the pixels. This data is presented as a single slice of the plasma density (figure 3) and as the full 3D plasma density with the same number of slices as the final calculation for comparison (figure 4 for the Gaussian and see figure 9 for the real plasma density).

6 Results of Data Taking

Whilst the project was coding focused I had ample opportunity to work with the FLA group in the control room for FLASHForward for data taking. These results are based on 100 scanned points, equally spaced across the maximal travel distance of the delay stage. The laser characteristics are presented from the full data sample and whilst the plasma density was calculated for each slice only the first 10 are plotted due to MATLAB memory issues.

6.1 Laser Intensity Images

Laser intensity images were produced as illustrated in figure 5 for all scan locations over the beam path. From the image it is clear that the laser pulse is far from the example Gaussian intensity shown in figure 3.
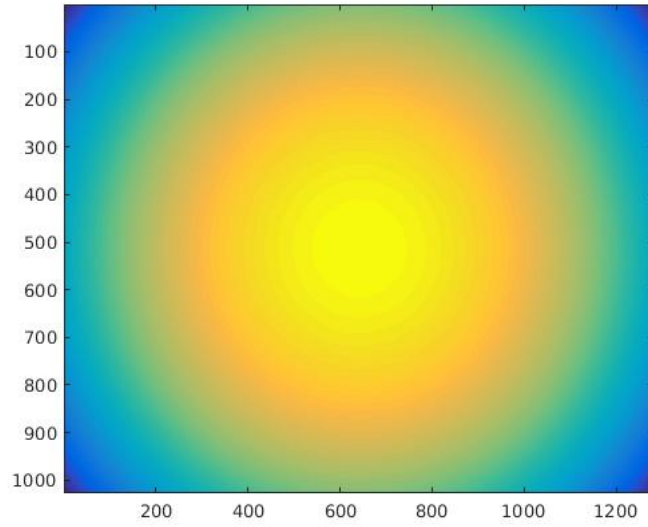
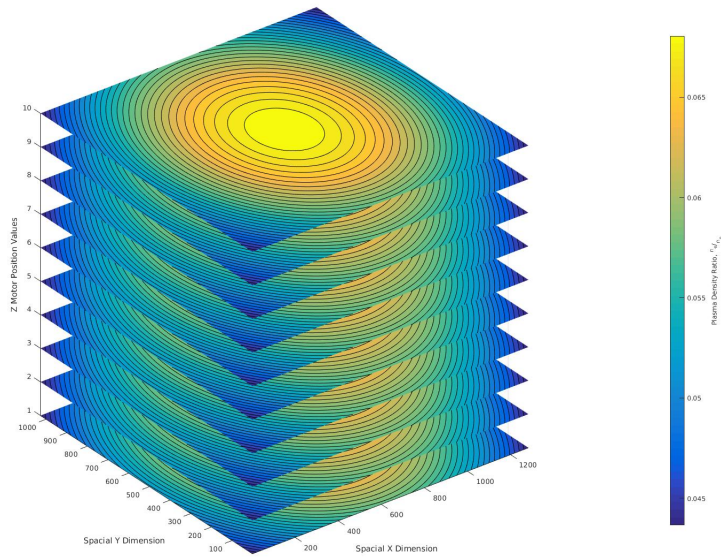Figure 3: The figure displays the Gaussian intensity profile used for the example process in the code.

Figure 4: The figure displays the 3D plasma density distribution as calculated using the Gaussian intensity data

6.2 Laser Intensity with Axial Projections

6.3 Spacial σ_x and σ_y Plots

The σ_x and σ_y values were calculated at all scan locations and plotted (figure 7). There is no clear beam waist which would be expected. The coefficient of change (figure 8)

12
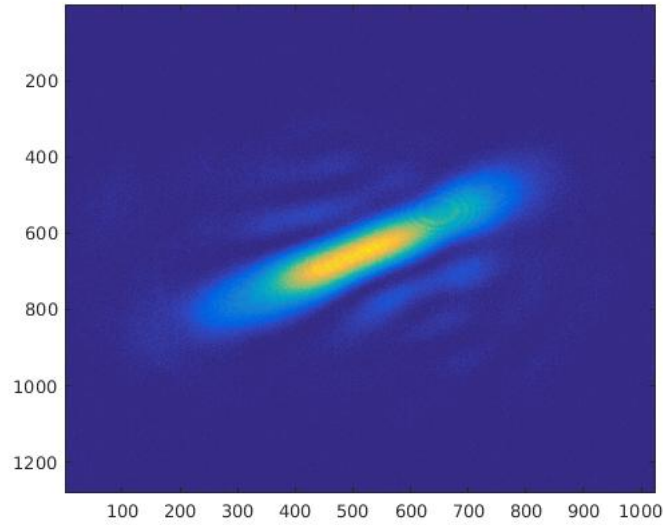
Figure 5: Intensity image produced by the camera at the centre of the scanning stage. The axis values indicate the pixel values. This is the intensity data used for the later calculations.
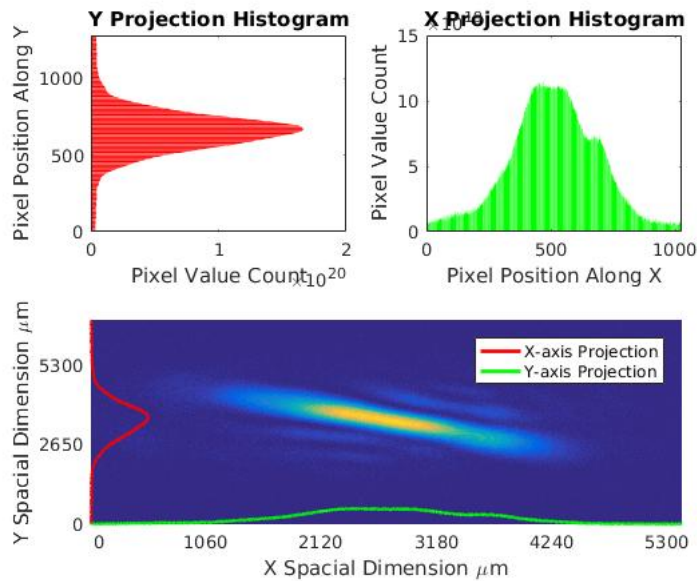

Figure 6: The upper plots show the pixel sum across the X and Y projections. These are absolute values whilst the corresponding lines on the lower plot have been scaled to the image and are for illustration purposes only. They are plotted on top of the intensity image.

was then calculated to see if this would provide more clarity in terms of beam shape but this was not successful.
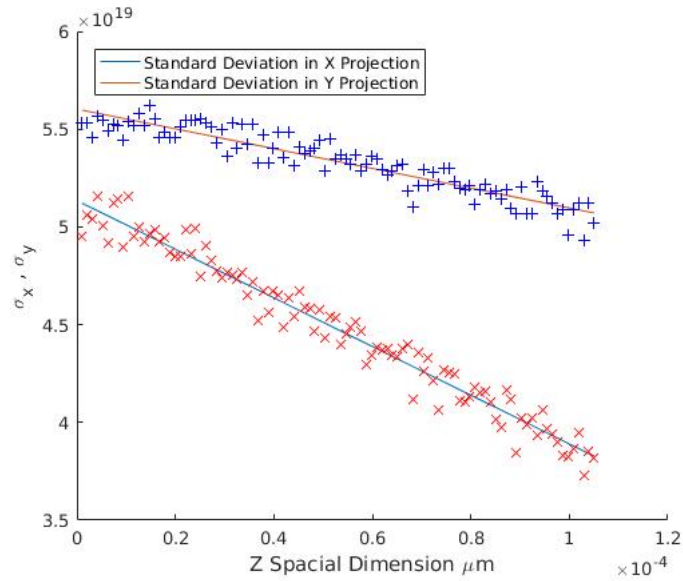
13

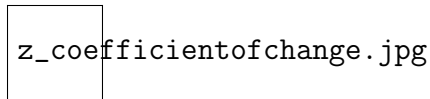Figure 7: The standard deviation in both the x and y directions is plotted over the scanning range.

z_coefficientofchange.jpg

Figure 8: This figure plots the coefficient of change over the scanning range.

6.4 M^2 Laser Values

These results were obtained for the the x and y directions separately due to the asymmetry in the beam. Sadly the code ceased working in the final week of the project and I have been currently unable to fix this. Calculated values will be sent to the FLA group as soon as the fix is completed.

6.5 Plasma Density Profile

The plasma density profile was successfully calculated for 10 out of the possible 100 real intensity images due to the limitations of RAM and the large image sizes.
In comparison to the the three dimensional plasma density for the Gaussian example (figure 4) it is much more complex. Whilst the contour plots are still present they struggle to quantify areas of equal ionisation due to the pixel by pixel fluctuations present in real data which is absent from a Gaussian intensity plot.
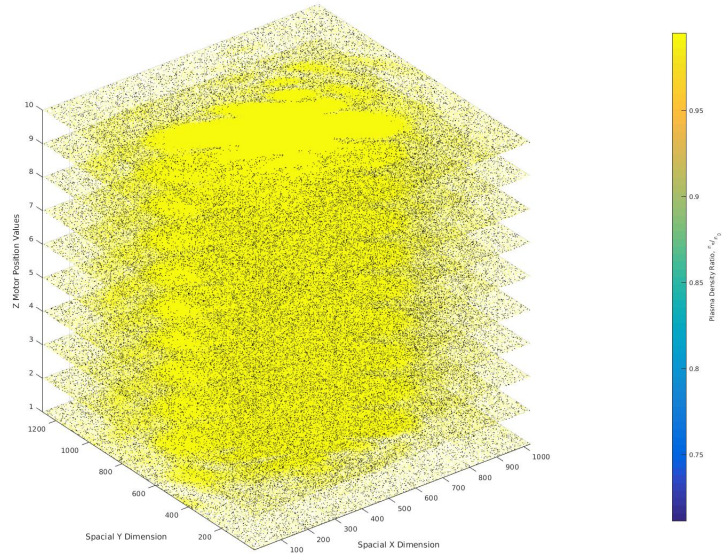
14

Figure 9: The final 3D plasma density profile is shown. This plot shows only 10 out of the 100 scans taken.

7 Future Project

During the PICO motor focusing routine only one of the two available PICO motors was used for focusing. In future the second PICO motor could be used in tandem with the first through a two point focusing method of improving the beam position and focus further after the beam is driven by the moving delay stage. One of the long term goals for FLASHForward is to investigate Trojan horse or Plasma Torch injection. To do this requires a mixture of gases. The ADK rate (see section 4.2.2) can be calculated separately for these two gases to confirm that they behave as expected under the ionisation of the laser. The laser was assumed to have zero dispersion throughout the gas. This could be modelled in future studies to confirm that this is a negligible effect or to model the plasma density of the cell more accurately by taking this into account. Finally, as the 3 dimensional plasma density profile is simply a concatenation of the 2 dimensional calculated slices it may be valuable to average the values between two slices to create a smooth. connected plasma density distribution. The addition of extra functions in the last week of the project led to the code crashing due to memory issues. This will be remedied as soon as possible and the plasma density images updated with the new data.

8 Conclusion

A MATLAB script was created with the purpose of automatic intensity data taking at the longitudinal beam diagnostics at FLASHForward. This data was then used to characterise the laser beam and create a plasma density profile successfully. The script
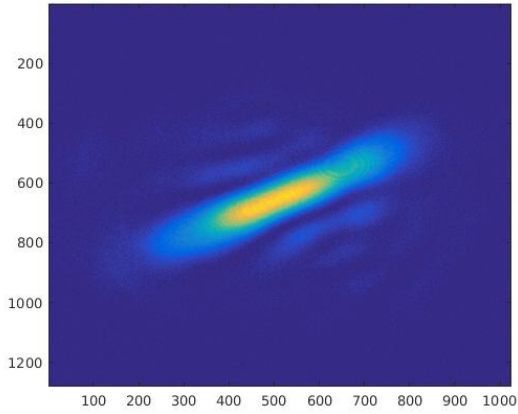
(a) Laser intensity profile
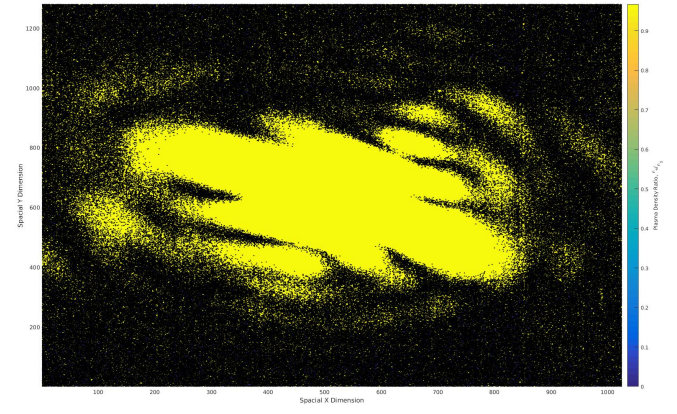
(b) Plasma density profile

Figure 10: A comparison between the intensity image taken by the camera in the longitudinal laser diagnostics and the plasma density profile calculated for these values. This data was taken with the delay stage closest to the OWIS motor.

allows for a large range of user preferences through the changing of single "choice" variables at the beginning of the script thus allowing the code to take on a large number of roles within the future of FLASHForward.

9 Acknowledgements

I would like to take this time to thank the many people that have provided assistance and made this a thoroughly enjoyable experience throughout my stay at DESY. Firstly my supervisor Alexander Knetsch has constantly provided help and support throughout my time here. Alex and the whole FLA team have made me feel very welcome at all times and provided me with help on any questions I may have. The skills I have learned here will be invaluable in my future career and I could not be more thankful for that. It has been a great 8 weeks full of challenges, meeting new people and exploring Hamburg. I would thoroughly recommend a summer project at DESY to anyone.

References

[1] J Grebenyuk, A Martinez de la Ossa, T Mehrling, and J Osterhoff. Beam-driven plasma-based acceleration of electrons with density down-ramp injection at flashforward. *Nuclear Instruments and Methods in Physics Research Section A: Accelerators, Spectrometers, Detectors and Associated Equipment*, 740:246–249, 2014.

[2] Erik Adli, Carl Andreas Lindstrøm, J Allen, CI Clarke, J Frederico, SJ Gessner, SZ Green, MJ Hogan, MD Litos, B OShea, et al. Long-range attraction of an ultrarelativistic electron beam by a column of neutral plasma. *New Journal of Physics*, 18(10):103013, 2016.

[3] A Aschikhin, C Behrens, S Bohlen, J Dale, N Delbos, L Di Lucchio, E Elsen, J-H Erbe, M Felber, B Foster, et al. The flashforward facility at desy. *Nuclear Instruments and Methods in Physics Research Section A: Accelerators, Spectrometers, Detectors and Associated Equipment*, 806:175–183, 2016.

[4] Ishkhan Gorgisyan, Chiara Bracco, Stephane Burger, Michele Cascella, Steffen Döbert, Spencer Gessner, Edda Gschwendtner, Lars Jensen, Steen Jensen, Simon Jolly, et al. Commissioning of beam instrumentation at the cern awake facility after integration of the electron beam line. In *9th Int. Particle Accelerator Conf.(IPAC'18), Vancouver, BC, Canada, April 29-May 4, 2018*, pages 1993–1996. JACOW Publishing, Geneva, Switzerland, 2018.

[5] MV Ammosov. Tunnel ionization of complex atoms and of atomic ions in an altemating electromagnetic field. *Sov. Phys. JETP*, 64:1191, 1987.

[6] D. Bauer and P. Mulser. Exact field ionization rates in the barrier-suppression regime from numerical time-dependent schrödinger-equation calculations. *Phys. Rev. A*, 59:569–577, Jan 1999.

[7] David L Bruhwiler, DA Dimitrov, John R Cary, Eric Esarey, Wim Leemans, and Rodolfo E Giacone. Particle-in-cell simulations of tunneling ionization effects in plasma-based accelerators. *Physics of Plasmas*, 10(5):2022–2030, 2003.

[8] Alexander Knetsch. Acceleration of laser-injected electron beams in an electron-beam driven plasma wakefield accelerator. Technical report, Verlag Deutsches Elektronen-Synchrotron, 2018.

[9] Anthony E Siegman. How to (maybe) measure laser beam quality. In *Diode Pumped Solid State Lasers: Applications and Issues*, page MQ1. Optical Society of America, 1998.

[10] Rdiger Paschotta. Beam parameter product, Oct 2017.